Root-Growth Mechanism for Single-Wall Carbon Nanotubes

J. Gavillet,[1] A. Loiseau,[1] C. Journet,[2] F. Willaime,[3] F. Ducastelle,[1] and J.-C. Charlier[4]

[1]*Laboratoire d'Etude des Microstructures (LEM), ONERA-CNRS, BP72, 92322 Châtillon Cedex, France*
[2]*Département de Physique des Matériaux (DPM), Université Claude Bernard Lyon 1, 69622 Villeurbanne Cedex, France*
[3]*Section de Recherches de Métallurgie Physique (SRMP), CEA/Saclay, 91191 Gif-sur-Yvette, France*
[4]*Unité PCPM, Université Catholique de Louvain, Place Croix du Sud 1, 1348 Louvain-la Neuve, Belgique*

(Received 11 December 2000; published 10 December 2001)

The catalytic growth of single-wall carbon nanotubes is investigated by high-resolution transmission electron microscopy. The similarities between the samples synthesized from different techniques suggest a common growth mechanism based on a vapor-liquid-solid model. Quantum-molecular-dynamics simulations support a root growth mechanism where carbon atoms are incorporated into the tube base by a diffusion-segregation process.

DOI: 10.1103/PhysRevLett.87.275504 PACS numbers: 61.48.+c, 68.37.Lp, 81.10.Aj

Single-wall carbon nanotubes (SWNTs) are currently the subject of intense research efforts. The growth of SWNTs differs from that of multishell tubes insofar as catalysts are necessary for their formation. In order to optimize their yield and quality, several production methods have been used for their synthesis. Single-wall nanotubes can be produced by arc discharge [1], laser ablation [2], and solar furnaces [3], which are high temperature processes and catalytic methods [4,5], which are medium temperature syntheses ($\sim$1500 K). In the high temperature techniques, the carbon and catalyst are evaporated simultaneously at about 4000 K but the formation of nanotubes most probably occurs at lower temperatures ($\sim$1500 K also) as discussed below; see also Refs. [6,7]. In the catalytic methods, the carbon source is obtained from the decomposition of a gas phase (CO, methane, ethylene, etc.) by small metallic particles covering a substrate. Although these techniques involve different temperature ranges, they present strong analogies.

(i) For all synthesis techniques, transition and rare earth metals, such as Ni, Co, Fe, Y, La and more efficient mixtures of them [8], are found to be the best elements to catalyze SWNT formation.

(ii) The morphologies of the SWNTs produced by the different techniques are very similar. In each case, SWNTs can be found isolated or self-assembled in crystalline bundles, their diameters varying from 0.7 to 3 nm. These correlations suggest that a common mechanism could explain the growth of SWNTs.

Although the metal-catalytic growth of SWNTs is still a debated issue, it is believed to proceed via solvation of carbon vapor into metal clusters, followed by precipitation of carbon excess in the form of nanotubes [9,10]. From experimental observations, two distinct situations seem to arise depending on the size of the catalytic particle. When the metal particle diameter is of the order of a few tens of nm, the precipitation of a large number of SWNTs from its surface is observed [9,11]. The maximum yield is always obtained for synthesis parameters giving rise to a size distribution of metallic nanoparticles centered on 15 nm. When it is below 5 nm, the particle is frequently found trapped in the tip of SWNTs [12], and the diameter of the SWNTs is directly related to the particle size. These observations support a model of growth by chemisorption from the vapor phase proposed long ago for carbon filaments [13,14]. Another possibility which has been put forward is that the catalytic metal particle can be reduced to a few atoms at the tip of the nanotube, either preventing its closure by scooting around and stabilizing the reactive dangling bonds [2] or leading the tip to remain chemically active and act as attraction sites for carbon adatoms [15]. Finally, it has also been suggested that preformed fullerenes could play the role of nucleation seeds [6].

In this Letter, we investigate the nucleation and growth of SWNTs, where carbon atoms precipitate from particles larger than the tube diameter. Such a process, which implies a root-growth mechanism, is studied using both high-resolution transmission electron microscopy (HRTEM) and quantum-molecular-dynamics simulations. We will show that carbon atoms can be added at the root of a growing tube by a diffusion-segregation process occurring at the surface of the catalytic particle.

Since few results are available in the literature concerning this point, we first performed careful HRTEM studies (using a Jeol 4000FX microscope) of long SWNT bundle extremities of samples produced by arc discharge [1], laser ablation [2,16], and catalytic decomposition [12] (an example is shown in Fig. 1). The observations have been

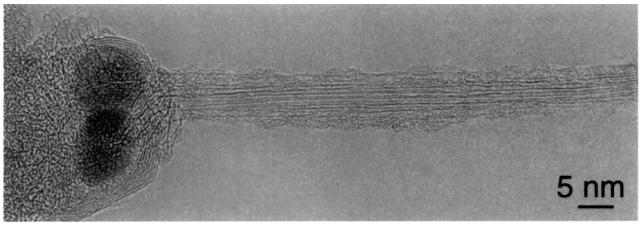

FIG. 1. HRTEM image of a long SWNT bundle emanating from a 10 nm metallic Ni-Y particle. The bundle was synthesized by the electric arc method described in [1].

compared with those made on samples obtained by solar energy [3]. For all these production methods, the basic result is the same: SWNT bundles have one free extremity and the other is attached to small metallic nanoparticles. Whatever the technique used, bundles emerge from nanoparticles of typically 15 nm. When the SWNT bundles are short (<40 nm), the two extremities are observed simultaneously and the junction between the bundle and the nanoparticle is obvious (Figs. 2 and 3). The free part of the bundle shows a closed and empty end, whereas the other is linked to the nanoparticle and can also be embedded in amorphous carbon (Fig. 3b).

In some cases, bundle embryos (Fig. 2a) or nuclei of individual nanotubes (Fig. 2b) have clearly been identified. These observations show that nanotube roots are attached to metallic nanoparticles. Short ropes, i.e., intermediate situations between nuclei and long SWNT bundles, can also be observed. Figure 3a clearly shows that short ropes emerge from the nanoparticles and are fixed on them. In Fig. 3b, short ropes and their nanoparticles are also embedded in amorphous carbon.

To explain the key role played by the metal catalyst, we propose a mechanism, which adopts the concepts of the vapor-liquid-solid (VLS) model introduced in the 1960s to explain the growth of silicon whiskers [17]. This model, first proposed by Saito *et al.* [9] to explain the formation of sea-urchin–like structures, is extended here to the formation of SWNTs, isolated or in bundles, emerging from large catalytic particles.

Figure 4 presents a simplified sketch of the proposed scenario. The first step of the process is the formation of a liquid nanoparticle of metal supersaturated with carbon (Fig. 4a). These nanoparticles originate from plasma/vapor condensation in the moderate temperature zone of the arc discharge or laser ablation chamber. The nanoparticle size is determined by the reaction parameters such as temperature gradients, gas pressure, gas flux, etc. In the catalytic technique, the nanoparticles are produced before the SWNT synthesis and their size depends on the type of method used to disperse the catalyst on the substrate. The supersaturation is generated by decomposition and absorption of carbonaceous structures on the surface of the nanoparticles [4,5]. During the synthesis, the liquid nanoparticle is able to incorporate a large amount of carbon (the Ni-C phase diagram gives a maximum carbon solubility of 25%). Upon cooling, the solubility limit of carbon decreases and therefore carbon atoms start to segregate towards the surface. This effect increases when the temperature decreases and is maximum close to the solidification point, i.e., at temperatures about 1500 K. The occurrence of such a segregation process is also supported by the absence of carbon inside the nanoparticles [18]. At this stage, there is a competition between the formation of a graphitic sheet (Fig. 4b) and the nucleation of single-wall nanotubes (Fig. 4c).

Since the equilibrium structure is most probably a nanoparticle surrounded by a graphitic shell, the hypothesis now is that, in some cases, surface instabilities occur leading to the nucleation of tube tips such as, for example, those described by Maiti *et al.* [10]. One can imagine dynamic instabilities as those involved in the formation of dendrites in solidification processes or quasistatic instabilities similar to those involved in crystal growth produced by molecular beam epitaxy deposition [19]. The latter analogy is very appealing indeed if one replaces the deposition flux by a carbon segregation flux. The equivalent of a layer-by-layer growth (or Frank–van der Merwe process) would be here the formation of graphitic sheets, whereas the formation of islands (Volmer-Weber or Stranski-Krastanov processes) would be equivalent to the growth of nanotubes. If this analogy is correct, the different interface energies which determine the wetting properties of the nanoparticle surface should be important control parameters. Clearly, more detailed studies are required to test this type of thermodynamical model. Similar ideas have been put forward by Kanzow *et al.* [20].

Let us now comment on the final steps of the growth process depicted in Fig. 4. Once the nanotube nuclei are formed, growth should proceed through further incorporation of carbon at the root. In order to obtain long

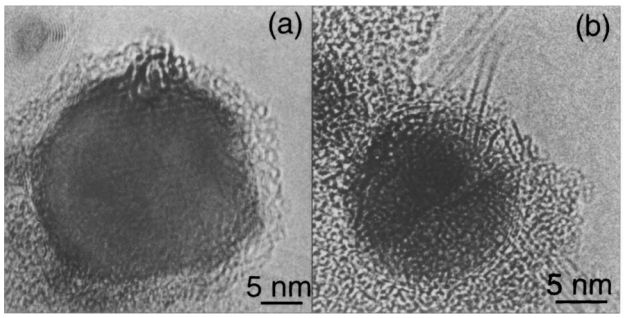

FIG. 2. (a) HRTEM image of an embryo of a SWNT bundle emerging from a metallic nanoparticle. SWNTs are seen as elongated caps, having a length between 3 and 5 nm. (b) HRTEM image of an individual nanotube fixed at the particle. Its free extremity vibrates in the electron beam, hence its diffuse contrast.

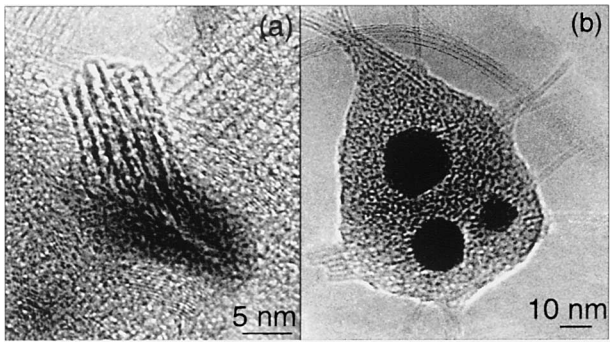

FIG. 3. HRTEM images of different short ropes attached to metallic particles. In (a) the rope is strongly inclined with respect to the electron beam; in (b) the rope and its particle are embedded in an amorphous carbon flake.

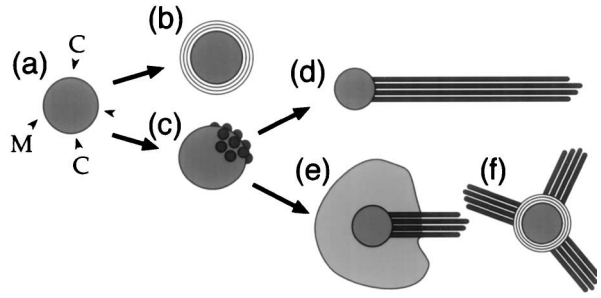

FIG. 4. Scenario, derived from the VLS model, for the nucleation and growth of SWNT ropes. See text.

nanotubes (Fig. 4d), the root-growth process should continue for a sufficiently long time, until local temperatures are too low, leading to the solidification of the nanoparticles. The development of nanotube embryos can also abort: Figures 4e and 4f schematize such situations. Corresponding observations are shown in Fig. 3. Nucleation did occur but growth did not take place so that carbon has partly condensed into amorphous carbon flakes or into a few graphitic layers.

To go beyond this phenomenological approach we have investigated the metal-carbon segregation process at the atomic level using quantum molecular dynamics (QMD) [21]. In this approach, the forces acting on the atoms are derived from the instantaneous electronic ground state, which is accurately described within density functional theory in the local density approximation. A 153 atom mixed Co-C cluster was created by extracting a sphere 1.3 nm in diameter from a hexagonal close-packed (HCP) Co structure, and by replacing randomly two-thirds of the Co atoms by C atoms (Fig. 5). The mixed cluster was then placed in a supercell [22], and heated up to 2000 K by means of a Nosé-Hoover thermostat [23] (Fig. 5a). After a thermalization period of 5 ps at 2000 K, the temperature was gradually decreased to 1500 K using a thermal gradient of 100 K/ps. After 5 ps at 1500 K, most

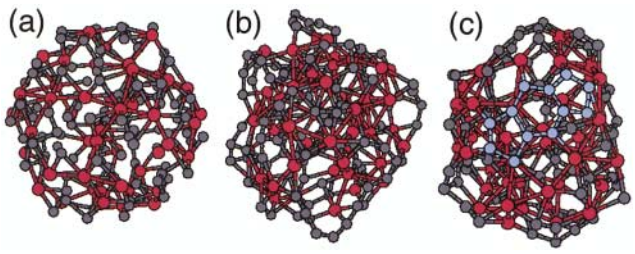

FIG. 5 (color). Segregation process in a cluster containing 51 Co atoms (big red spheres) and 102 C atoms (smaller grey spheres) when the temperature drops from 2000 to 1500 K. (a) The cluster is first heated up to 2000 K, leading to a homogeneous distribution of Co and C within the sphere volume. (b) The temperature is gradually decreased to 1500 K. C atoms segregate to the surface while Co atoms migrate to the center. (c) Carbon linear chains and aromatic rings (in blue) are created at the surface of the cluster. Total simulation time: 25 ps.

of the C atoms (~80%) segregate to the surface of the cluster, while the Co atoms migrate to its center (Fig. 5b). The C atoms at the surface move very quickly and form a network composed of connected linear chains and some aromatic rings. The creation of a hexagon connected to two pentagons is remarkable (Fig. 5c) and can be considered as a first stage of the nucleation process. However, the extremely long simulation times made it impossible to examine if these pentagons are preserved or if they become hexagons by incorporation of further carbon atoms. These quantum molecular dynamics simulations for systems

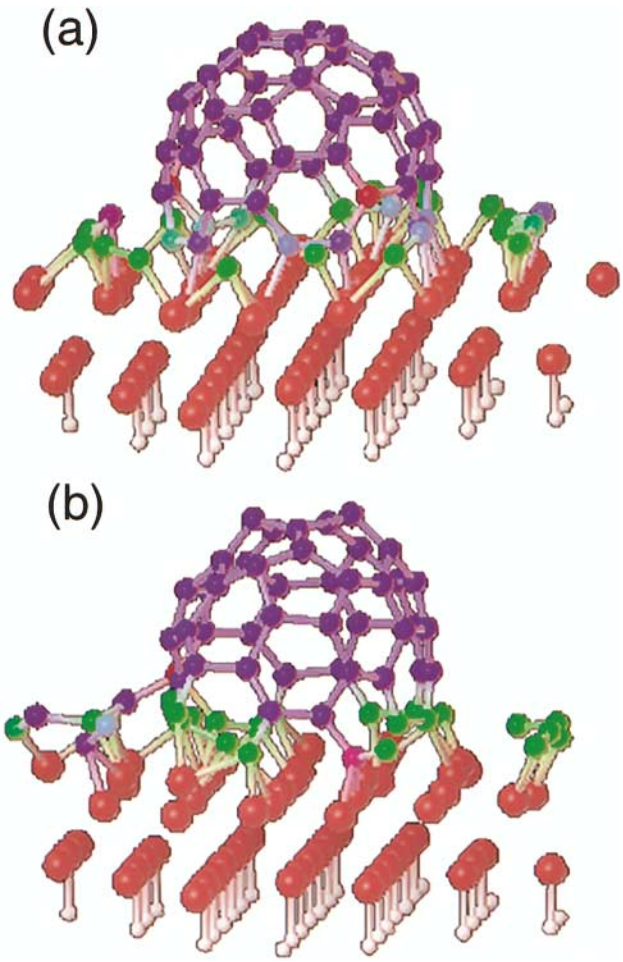

FIG. 6 (color). Root growth mechanism for SWNTs extruded from large catalytic nanoparticles. A small (6, 6) nanotube portion capped by a perfect fullerenelike hemisphere is placed on a slab of HCP Co, with 20 additional isolated carbon atoms on the particle surface. The model contains 74 carbon atoms (violet, green, or red spheres depending on the coordination: 4, 3, and 2, respectively), 59 cobalt atom (big red sphere), and 30 hydrogen atoms (small white spheres) terminating the metal particle. Coordinations between 2 (green) and 3 (violet) are represented by sky-blue spheres. The hydrogen atoms and the last layer of Co were kept fixed during the simulation. (a) Starting configuration at 0 K. (b) Incorporation into the honeycomb network of the nanotube root of five extra carbon atoms which have diffused on the nanoparticle surface at 1500 K. Total simulation time: 15 ps.

exceeding one hundred atoms are actually at the limit of what is possible to do on present computers.

The second step of the simulation consists of modeling the migration of carbon atoms at the surface of a catalyst particle and their incorporation to the SWNT base, thereby leading to a root growth mechanism. Figure 6 represents a SWNT closed at one end by half a C_{60} molecule while the reactive open part is deposited on a double layer of HCP cobalt, satisfying most of the dangling bonds (Fig. 6a). Twenty carbon atoms have been added at the surface of the metal particle in order to observe a migration process to the root of the nanotube. The global system is then heated up to 1500 K by means of a Nosé-Hoover thermostat [23]. After 15 ps of simulation, five carbon atoms had diffused to the tube base and were incorporated into the nanotube body (Fig. 6b). Even if the time scale of such simulations prevents us from studying the further evolution of the root growth, this incorporation as well as the absence of formation of a closed fullerenelike molecule suggest that this root growth mechanism is a good candidate to explain the emergence of carbon nanotubes from a large metal catalyst particle. Our QMD simulation shows that the role of the catalyst is not only to stabilize the forming tube but also to provide fluctuating Co-C bonds in the middle of which new carbon atoms are easily incorporated. This result contrasts with classical simulations, where a nanotube protrusion can grow out of a flat all-hexagonal graphene sheet by a root mechanism involving the presence of defects (heptagons) at the tube base to allow the incorporation of migrating carbon into the hexagonal network [10].

In summary, we have provided experimental and theoretical arguments in favor of a root-growth mechanism for single-wall nanotubes. Since the QMD simulations are extremely time and memory consuming, they cannot be used in a systematic manner to increase the length and time scales and to vary relevant parameters. Simplified models using tight-binding potentials are currently under development to undertake appropriate large scale simulations.

We acknowledge the group of P. Bernier (University of Montpellier II, France) for its assistance in the synthesis of arc discharge samples, J.-L. Cochon and D. Pigache (ONERA, Châtillon, France) for providing the laser ablation samples, and Dr. X. Blase, Dr. A. DeVita, and Professor R. Car for scientific discussions undertaken at the early stage of our work. J.-C. C. acknowledges the FNRS of Belgium for financial support. Part of this work was carried out within the Belgian Unteruniversity Project (PAI P4/10) and two EU projects (Contracts No. G5RD-CT-1999-00173 and No. HPRN-CT-2000-00128).

[1] C. Journet *et al.,* Nature (London) **388**, 756 (1997).
[2] A. Thess *et al.,* Science **273**, 483 (1996).
[3] L. Alvarez *et al.,* Appl. Phys. A **70**, 169 (2000).
[4] H. M. Cheng *et al.,* Appl. Phys. Lett. **72**, 3282 (1998).
[5] J. F. Colomer *et al.,* Chem. Commun. **14**, 1343 (1999); Chem. Phys. Lett. **317**, 83 (1990).
[6] H. Kataura *et al.,* Carbon **38**, 1691 (2000).
[7] O. Jost *et al.,* Appl. Phys. Lett. **75**, 2217 (1999).
[8] S. Seraphin and D. Zhou, Appl. Phys. Lett. **64**, 2087 (1994).
[9] Y. Saito *et al.,* Jpn. J. Appl. Phys. **33**, 526 (1994); Carbon **33**, 979 (1995).
[10] A. Maiti, C. J. Brabec, and J. Bernholc, Phys. Rev. B **55**, R6097 (1997).
[11] D. Zhou, S. Seraphin, and S. Wang, Appl. Phys. Lett. **65**, 1593 (1994).
[12] H. Dai *et al.,* Chem. Phys. Lett. **260**, 471 (1996).
[13] A. Oberlin, M. Endo, and T. Koyama, J. Cryst. Growth **32**, 335 (1976).
[14] G. G. Tibbetts, J. Cryst. Growth **66**, 632 (1984).
[15] J.-C. Charlier *et al.* (to be published).
[16] J.-L. Cochon *et al.,* in *Electronic Properties of Novel Materials,* edited by H. Kuzmany *et al.,* AIP Conf. Proc. No. 486 (AIP, New York, 1999), p. 237.
[17] R. S. Wagner and W. C. Ellis, Appl. Phys. Lett. **4**, 89 (1964).
[18] J. Gavillet *et al.,* in *Electronic Properties of Novel Materials,* edited by H. Kuzmany *et al.,* AIP Conf. Proc. No. 544 (AIP, New York, 2000), p. 222.
[19] A. Zangwill, *Physics at Surfaces* (Cambridge University Press, Cambridge, 1988).
[20] H. Kanzow *et al.,* Phys. Rev. B **60**, 11 180 (1999); Phys. Rev. B **63**, 125402 (2001).
[21] R. Car and M. Parrinello, Phys. Rev. Lett. **55**, 2471 (1985).
[22] The interaction between valence electrons and ionic cores was described using Troullier-Martins norm-conserving pseudopotentials. Periodic boundary conditions were adopted, keeping a minimum 7 Å distance between repeated images. Electronic wave functions are expanded into plane waves with a kinetic energy cutoff of 60 Ry. The equations of motion were integrated using a time step of 0.7 fs.
[23] S. Nosé, J. Chem. Phys. **81**, 511 (1984); H. G. Hoover, Phys. Rev. A **31**, 1695 (1985).